

Dynamics of electronic transitions and frequency dependence of negative capacitance in semiconductor diodes under high forward bias

Kanika Bansal, Mohamed Henini, Marzook S. Alshammari, and Shouvik Datta

Citation: [Applied Physics Letters](#) **105**, 123503 (2014); doi: 10.1063/1.4896541

View online: <http://dx.doi.org/10.1063/1.4896541>

View Table of Contents: <http://scitation.aip.org/content/aip/journal/apl/105/12?ver=pdfcov>

Published by the [AIP Publishing](#)

Articles you may be interested in

[Analysis of carrier transport and carrier trapping in organic diodes with polyimide-6,13-Bis\(triisopropylsilylethynyl\)pentacene double-layer by charge modulation spectroscopy and optical second harmonic generation measurement](#)

Appl. Phys. Lett. **105**, 073301 (2014); 10.1063/1.4893760

[Electroluminescence and capacitance-voltage characteristics of single-crystal n-type AlN \(0001\)/p-type diamond \(111\) heterojunction diodes](#)

Appl. Phys. Lett. **98**, 011908 (2011); 10.1063/1.3533380

[Temperature-dependent transition from injection-limited to space-charge-limited current in metal-organic diodes](#)

Appl. Phys. Lett. **95**, 143303 (2009); 10.1063/1.3243844

[Capacitance-voltage characterization of polyfluorene-based metal-insulator-semiconductor diodes](#)

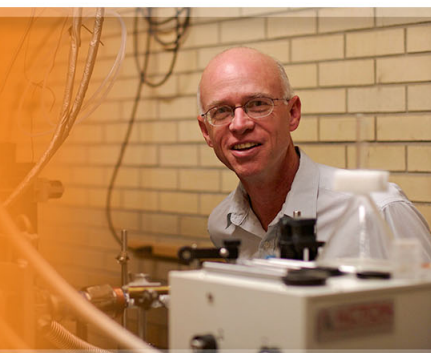
Appl. Phys. Lett. **89**, 013506 (2006); 10.1063/1.2219147

[The Meyer-Neldel rule for diodes in forward bias](#)

J. Appl. Phys. **96**, 7379 (2004); 10.1063/1.1818353



is pleased to announce **Reuben Collins**
as its new Editor-in-Chief



Dynamics of electronic transitions and frequency dependence of negative capacitance in semiconductor diodes under high forward bias

Kanika Bansal,¹ Mohamed Henini,² Marzook S. Alshammari,³ and Shouvik Datta¹

¹Division of Physics, Indian Institute of Science Education and Research, Pune 411008, Maharashtra, India

²Nottingham Nanotechnology and Nanoscience Centre, School of Physics and Astronomy, University of Nottingham, Nottingham NG7 2RD, United Kingdom

³The National Center of Nanotechnology, KACST, Riyadh 11442, Saudi Arabia

(Received 20 June 2014; accepted 14 September 2014; published online 24 September 2014)

We observed qualitatively dissimilar frequency dependence of negative capacitance under high charge injection in two sets of functionally different junction diodes: III-V based light emitting and Si-based non-light emitting diodes. Using an advanced approach based on bias activated differential capacitance, we developed a generalized understanding of negative capacitance phenomenon which can be extended to any diode based device structure. We explained the observations as the mutual competition of fast and slow electronic transition rates which are different in different devices. This study can be useful in understanding the interfacial effects in semiconductor heterostructures and may lead to superior device functionality. © 2014 AIP Publishing LLC.

[<http://dx.doi.org/10.1063/1.4896541>]

Even after decades of research in the field of semiconductors, behavior of a semiconductor junction diode under high forward bias is not fully understood. Junction diodes make the basis of a vast variety of devices which are an integral part of technology and consumers applications. Some of these diodes, such as light emitting diodes (LED) and laser diodes (LD), can function only under high forward bias. Hence, it becomes important to understand the electrical impedance of these diodes under such high forward bias not only to gain knowledge about the physical processes they undergo but also to make them more useful in various applications. In our previous studies,¹⁻⁴ we investigated the impedance of electroluminescent diodes (LEDs and LDs) under charge carrier injection. We observed that as the forward bias increases, the reactive component of the impedance demonstrates negative capacitance (NC). Higher magnitude of this NC for lower applied modulation frequencies has also been observed by many groups in electroluminescent devices⁵⁻⁷ and also in other semiconductor devices.^{8,9}

Here, we report qualitatively opposite dynamic behavior of NC in two sets of diodes with different functionalities: (a) III-V based electroluminescent diodes (ELDs): (i) InGaAs based quantum dot laser (QDL) diodes grown by Molecular Beam Epitaxy (MBE) on (100) GaAs substrates. A 0.7 μm -thick GaAs buffer layer was grown before deposition of the $\text{In}_{0.5}\text{Ga}_{0.5}\text{As}$ strained layer at 450 °C. The structure was completed with a 25 nm GaAs cap. Further details can be found in Ref. 10. (ii) Commercially purchased AlGaInP based quantum well laser (QWL) diodes from Sanyo (component No. DL 3148-025). These are edge emitting strained multi-quantum well structures (details can be found in Ref. 1), and (b) Si-based non-luminescent diodes: commercially purchased standard Si-based diodes 1N 4001, 1N 4007, and p-i-n photo diode SFH 213 from OSRAM Opto Semiconductors. The modulation frequency dependence of negative capacitance in Si diodes was found to be different than that of ELDs. We developed the analysis based on the frequency derivative of capacitance to probe such difference.

We came up with a generalized understanding of negative capacitance as a mutual competition of two rate-limited processes to explain the observations.

Figure 1(a) shows variation of measured small signal capacitance (C , using precision LCR meter E4980A from Agilent) with forward bias for QWL at different modulation frequencies. As the bias (V_{dc}) increases, the capacitance becomes negative and in the log scale, the frequency response curve terminates. With lower applied modulation frequency, the onset of negative capacitance occurs at lower forward biases. On the other hand, Figure 1(b) shows such capacitance voltage plots for Si diode (1N 4001) under forward bias. Frequency dependence of negative capacitance is completely reversed in this case. As the frequency decreases, we observe negative capacitance onset to shift towards higher applied injection levels. We also measured such negative capacitances in other Si based diodes (p-i-n photo diode SFH 213 and 1N 4007), all of which gave qualitatively similar frequency dependence.

In our earlier studies,^{1,2} to explain the occurrence of negative capacitance in ELDs, we considered the mutual competitive dynamics of sub-band gap defect levels and radiative recombination of available charge reservoir at high injection levels. Depending upon the applied modulation frequency and temperature of the device, defects within a certain energy depth E_{Th} can respond¹ to the applied signal and contribute to the measured impedance. Hence, one can write the standard expression relating E_{Th} , thermal rate of charge carriers trapping and de-trapping from defect states (τ), and modulation frequency (f) as

$$f \approx \frac{1}{\tau} = \nu \exp\left(-\frac{E_{Th}}{k_B T}\right) \quad (1a)$$

or

$$E_{Th} = k_B T \ln(\nu/f), \quad (1b)$$

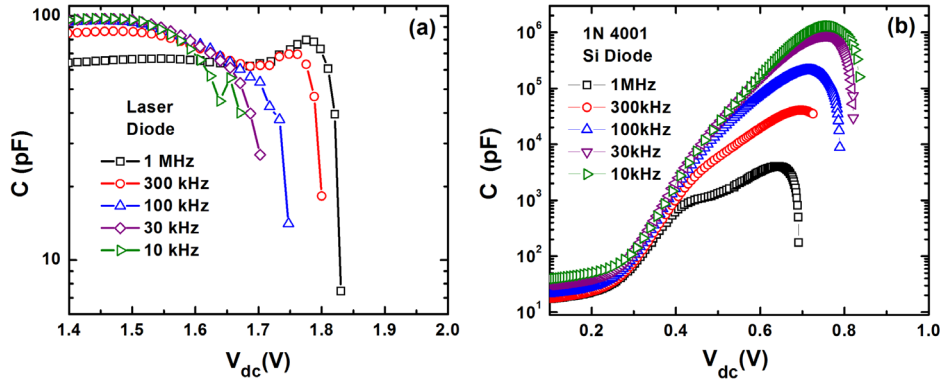


FIG. 1. Variation of capacitance with bias under different applied modulation frequencies for (a) quantum well laser diode (DL 3148-025) and (b) Si diode (1N 4001). The point where a particular data plot terminates is the starting point of negative capacitance. In Si diodes, high frequency produces negative capacitance for lower biases which is opposite to that of quantum well laser diodes.

where T is the temperature which we kept constant (296 ± 0.1 K) during the measurements, k_B is the Boltzmann constant, and ν is the thermal prefactor. When the applied modulation is comparable to $1/\tau$, we observe that the defect responds to the applied sinusoidal modulation which ultimately affects the measured impedance of the active junction.

In case of ELDs, the onset of light emission also interrupts the total number of charge carriers available at the junction which includes the contribution from defect levels ($n_{Trapped}$). Radiative recombination process consumes charge carriers coming out of the defect states irreversibly and faster than these are replenished. As a result, at the end of the modulation cycle, equilibrium defect population is not recovered. This can cause a transient change in the quasi Fermi level position and the carrier reservoir at the junction. To establish the equilibrium, a compensatory current is induced which lags behind the voltage. Consequently, we observe an “inductive like” reactance, experimentally measured as NC. The more is the contribution from defect levels ($n_{Trapped}$), the more compensation would be required to achieve such equilibrium. It is easy to understand from Eq. (1) that with decreasing frequency, E_{Th} increases. This increases $n_{Trapped}$ and hence the magnitude of compensatory current which ultimately increases the magnitude of NC at decreasing modulation frequencies, as observed in the past.^{1,2}

However, in case of non-luminescent Si-based diodes, such fast (\sim ps) radiative recombinations do not take place. Yet the occurrence of NC points towards the presence of mutually competing different rate-limited electronic processes with different time scales.

To further examine the dynamic dependence of NC on frequency, in Figure 2, we plot and compare the bias values

at which the NC starts to occur (V_{NC}) as a function of frequency f for two different types of diodes. In case of ELDs (Figure 2(a)), V_{NC} increases monotonically with increasing applied frequency. This behavior remains qualitatively the same for QWL and QDL diodes and is in accordance with the results reported by Feng *et al.*¹¹ It is important to note that the defect contribution can only be activated if defects exist below the quasi Fermi level in the band gap.¹ As we increase frequency, we decrease the depth E_{Th} , and hence the contribution from relatively deeper defects is lost. To overcome this, quasi Fermi level has to move towards the band edge to increase the effective defect contribution, which can be achieved by increasing the applied bias (at a constant temperature). Once the defect contribution is significant to compete with the radiative recombination process, we start observing NC. This is why we observe that as the modulation frequency increases, V_{NC} increases in ELDs.¹

On the other hand, as shown in Figure 2(b), for all the Si based non-luminescent devices investigated, V_{NC} does not follow a monotonic behavior with increasing f . Here, two different regions can be clearly identified depending upon the variation of V_{NC} with frequency. In region I, V_{NC} is relatively independent of applied modulation frequencies for lower frequency ranges below $\sim 5 \times 10^4$ Hz and remains relatively constant. In region II, above $\sim 5 \times 10^4$ Hz, V_{NC} decreases with increasing frequencies which is opposite of what is observed in the case of ELDs.

To understand this difference, we studied the frequency derivative of capacitance response. Usually, a peak in $f dC/df$ is observed with frequency or temperature variation corresponding to a position of maximum response from the defects or the position where quasi Fermi level crosses the respective defect energy level.^{12–14} In case of high charge

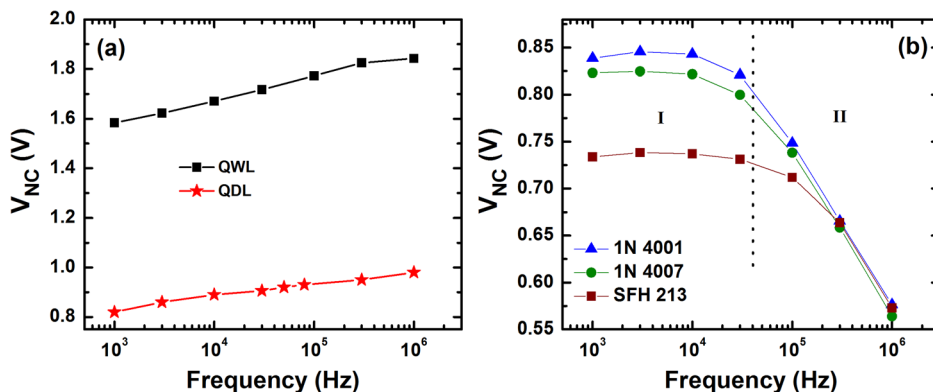


FIG. 2. Variation of the bias at which negative capacitance is observed (V_{NC}) for different applied modulation frequencies for (a) QWL and QDL diodes and (b) Si based diodes. For laser diodes, V_{NC} increases monotonically with increasing frequency. For Si diodes, V_{NC} first stays somewhat constant with increasing frequency range (region I) and then decreases with increasing frequencies (region II).

injection, which induces interesting NC behavior, we focus on the bias (V_{dc}) activated dynamics of rate processes at room temperature. Experiments show that⁴ this dependence of rate process on T and V_{dc} is mutually inverse and is expressed as $1/T = \eta V_{dc}$, where η is a proportionality constant for correct dimensionality. Equation (1) can then be modified to the form

$$f_{Max} \approx \nu \exp\left(-\frac{E_{Th}}{k_B} \eta V_{dc}\right), \quad (2)$$

where f_{Max} corresponds to the frequency of maximum response (in fdC/df vs f plot). Rewriting Eq. (2) gives $\ln f_{Max} = \ln \nu + \left(-\frac{E_{Th}}{k_B} \eta V_{dc}\right)$. To verify the validity of this equation, linear behavior of $\ln f_{Max}$ with V_{dc} is required, which we have demonstrated in case of ELDs.⁴ Thus, the slope (m) of the straight line is directly proportional to the thermal activation energy, i.e.,

$$m = \left(-\frac{E_{Th}}{k_B} \eta\right). \quad (3)$$

Figure 3(a) shows the variation of fdC/df for a wide range of applied modulation frequencies for Si diode 1N 4001. We observe two prominent peaks in the fdC/df vs f plot. This is fundamentally different from the differential capacitance response observed in case of ELDs, where only one peak was observed.⁴ As the bias increases, f_{Max} for both the peaks shifts to the respective lower frequency sides. This variation of $\ln f_{Max}$ with applied bias is plotted in Figure 3(b). Such linear variation of $\ln f_{Max}$ with V_{dc} validates our conceived equation (2). Values of the slopes are found to be -4.3 ± 0.1 for lower frequency and

-13.0 ± 0.3 for higher frequency response. This difference may be related to entropic contribution to free energy barrier for a particular electronic defect.¹⁵ Unlike ELDs,⁴ Si based diode structures do not show any sign change of slopes in $\ln f_{Max}$ vs V_{dc} plot, which were related to the presence of excitons during light emission. It is worth mentioning that the behavior of undifferentiated capacitance with frequency, as shown in Ref. 16, Figure S1 (supplementary material) matches well with the previously reported results on Si based photodetectors.¹⁷ Though the occurrence of NC is shown in that report, the frequency dependence has not been dealt with. In this letter, we elaborate on this less explored feature of NC for commonly available diodes, which otherwise show similar properties as per reported literature, by using the advanced technique and analyses we have developed.

Note that in these bias activated processes, as the modulation frequency reaches between $\sim 5 \times 10^4$ and 10^6 Hz, peak 2 starts to respond significantly only after 0.45 V. However, slower defect response (peak 1) starts appearing at much lower biases. The density of defects responding at such frequencies is directly proportional to the derivative fdC/df .^{12,15} Hence, the area under the peaks represents the density of defects within the energy range spanned by the corresponding range of modulation frequency. In Figure 3(c), we found that the area acquired by the right half of peak 1 (overlapping with peak 2) increases in correlation with the area acquired by peak 2. Net defect density of peak 1 is much larger as compared to peak 2. However, at large forward biases, the rate of increase in peak 2 is faster than that of peak 1. This can be viewed from the plot in the inset of Figure 3(c), where values are normalized with respect to the highest area value for respective peaks. We ascribe this observed correlation as

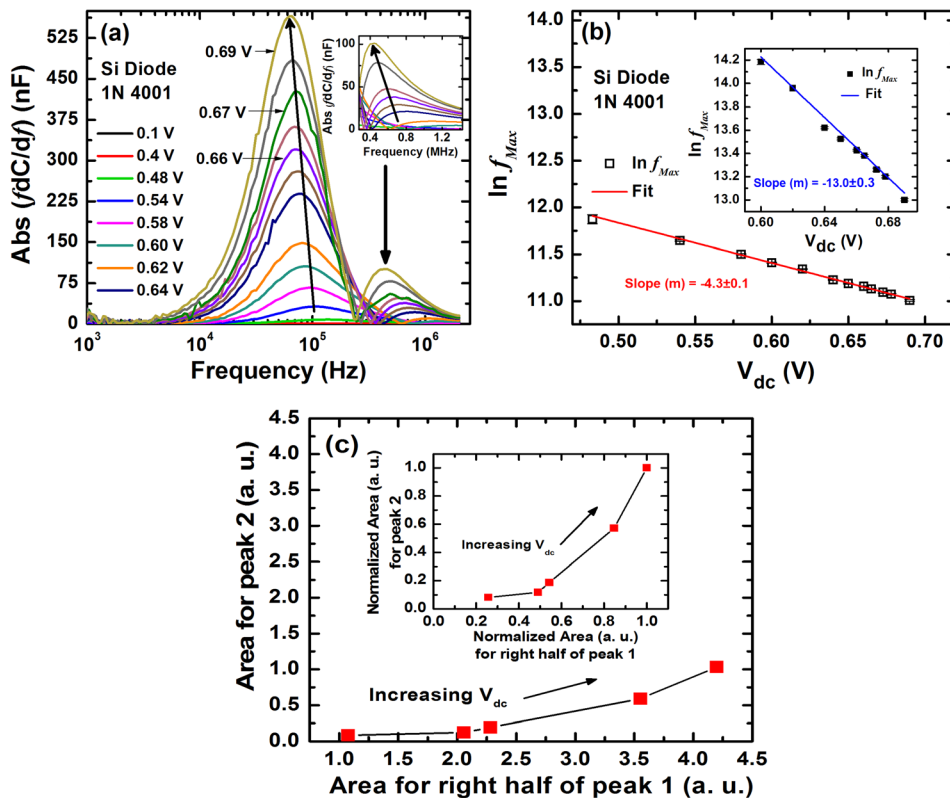


FIG. 3. (a) Absolute value of fdC/df showing two peaks at different frequency positions for Si diode. Peak frequency values are used to plot $\ln f_{Max}$ with applied bias (V_{dc}) as shown in (b). Inset in (b) shows the plot for the peaks at higher frequency side (peak 2). In both cases, peak frequency decreases with increasing bias. (c) The area under the right half of peak 1 and peak 2 increases with increasing bias in a correlated fashion. Inset shows the same plot normalized with respect to the largest area. Lines joining the data points are for visual clarity only.

an evidence for competition of two rate-limited processes governing the voltage onset of NC.

In Si diodes, two differently sized defect responses (bigger peak 1 and smaller peak 2) overlap (within similar frequency/energy ranges) and compete with each other for the overall impedance of the junction. At modulation frequencies $>5 \times 10^4$ Hz, the steady state situation is not fully recovered at the end of the sinusoidal modulation because the presence of a dominant and slower defect channel interrupts the dynamics of relatively smaller but faster defect response. This results in a mismatch of charge trapping and emission from these two defect channels over a complete cycle. Subsequently, a transient change in the charge carrier population coming from these defects can surface, giving rise to a compensatory current and hence the negative capacitance.^{1,2} In this region II of Figure 2(b), the contribution from relatively faster defect channels reduces with decreasing frequency. This requires further increase in the applied bias to generate significant contribution from shallower and faster channels which compete with slower channels to produce NC. As a result, V_{NC} increases with decreasing frequencies. However, this is qualitatively opposite to the case of ELDs¹ where fast and dominant radiative recombination irreversibly depletes the charge carrier reservoir competing with the much slower and smaller steady state defect response.

As we decrease the frequency below $\sim 5 \times 10^4$ Hz (region I, Figure 2(b)), we modulate the defects which only have slower component of thermal rate of carrier exchange with the band edge. However, until a significant intensity of bias is applied, which can activate the shallower defects (faster channels), we do not observe any NC effect. For high enough forward biases, contribution of faster channels again competes with the slower defect response and NC is observed. Since the activation of this high frequency defect response (peak 2) with increasing bias is not dependent on slower modulation frequencies, V_{NC} in region I of Figure 2(b) also does not vary much with changing modulation frequencies. Note that in some of the Si-based devices, it has been reported^{9,18} that the frequency dependence of NC is qualitatively similar to that of ELDs. We argue that this could be due to the interplay of different time scale processes in a manner similar to ELDs.

To summarize, we probed two functionally different diode structures and observed fundamentally different behavior of frequency dependent negative capacitance under high forward biases. We developed an alternate technique to

probe the device physics by measuring bias activated differential capacitance response (dC/dV) as a function of modulation frequency (f). Our analysis agrees well with the experimental results. In electroluminescent diodes, faster radiative recombination competes with slower and weaker defect response; however, in Si diodes, two overlapping defect channels of varied strength and time scales compete to cause negative capacitance. This study provides a generalized understanding of the electronic processes that give rise to negative capacitance response in junction diodes, which may lead to new device functionalities. To further optimize the device application, one can look into the details of a typical device structure, identifying the nature of particular electronic defects.

Authors wish to thank IISER-Pune for startup funding of the laboratory infrastructure as well as the Grant No. SR/S2/CMP-72/2012 from Department of Science and Technology, Government of India. K.B. is thankful to Council for Scientific and Industrial Research, India for senior research fellowship. M.H. acknowledges support from the UK Engineering and Physical Sciences Research Council.

¹K. Bansal and S. Datta, *J. Appl. Phys.* **110**, 114509 (2011).

²K. Bansal, *Phys. Status Solid C* **10**, 593 (2013).

³K. Bansal and S. Datta, *Appl. Phys. Lett.* **102**, 053508 (2013).

⁴K. Bansal and S. Datta, e-print [arXiv:1312.7259](https://arxiv.org/abs/1312.7259) [cond-mat.mes-hall].

⁵J. Bisquert, G. Garcia-Belmonte, A. Pitarch, and H. J. Bolink, *Chem. Phys. Lett.* **422**, 184 (2006).

⁶Y. Li, C. D. Wang, L. F. Feng, C. T. Zhu, H. X. Cong, D. Li, and G. Y. Zhang, *J. Appl. Phys.* **109**, 124506 (2011).

⁷L. F. Feng, D. Li, C. Y. Zhu, C. D. Wang, H. X. Cong, X. S. Xie, and C. Z. Lu, *J. Appl. Phys.* **102**, 063102 (2007).

⁸See Refs. 1–5, and work cited therein.

⁹M. Anutgan and I. Atilgan, *Appl. Phys. Lett.* **102**, 153504 (2013).

¹⁰A. Polimeni, M. Henini, A. Patane, L. Eaves, P. C. Main, and G. Hill, *Appl. Phys. Lett.* **73**, 1415 (1998).

¹¹L. F. Feng, Y. Li, D. Li, X. D. Hu, W. Yang, C. D. Wang, and Q. Y. Xing, *Appl. Phys. Lett.* **101**, 233506 (2012).

¹²T. Walter, R. Herberholz, C. Müller, and H. W. Schock, *J. Appl. Phys.* **80**, 4411 (1996).

¹³P. Boix, G. Garcia-Belmonte, U. Muñecas, M. Neophytou, C. Waldauf, and R. Pacios, *Appl. Phys. Lett.* **95**, 233302 (2009).

¹⁴J. V. Li and D. H. Levi, *J. Appl. Phys.* **109**, 083701 (2011).

¹⁵S. Datta, J. D. Cohen, Y. Xu, A. H. Mahan, and H. M. Branz, *J. Non-Cryst. Solids* **354**, 2126 (2008).

¹⁶See supplementary material at <http://dx.doi.org/10.1063/1.4896541> for capacitance vs modulation frequency at different biases for a Si diode.

¹⁷R. Gharbi, M. Abdelkrim, M. Fathallah, E. Tresso, S. Ferrero, C. F. Pirri, and T. Mohamed Brahim, *Solid State Electron.* **50**, 367 (2006).

¹⁸F. Lemmi and N. M. Johnson, *Appl. Phys. Lett.* **74**, 251 (1999).